Finite element modelling of fibre-reinforced brittle materials

Jyrki Kullaa*
Delft University of Technology, Delft
TNO Building and Construction Research, Rijswijk , The Netherlands

The tensile constitutive behaviour of fibre-reinforced brittle materials can be extended to two or three dimensions by using the finite element method with crack models. The three approaches in this study include the smeared and discrete crack concepts and a multi-surface plasticity model. The tensile relation represents the crack normal stress-normal strain behaviour. Depending on the fracture mode – single or multiple – different modelling strategies must be considered.
Applications in this study include a short steel fibre-reinforced densified small particles (DSP) beam, kevlar fibre-reinforced beams with and without ordinary reinforcing bars, and a steel fibre-reinforced concrete pipe. The increase of the peak load due to fibres could be reproduced, which supports the validity of the proposed method.
All the tensile relations have been computed from micromechanical properties. Some micromechanical properties have been obtained by trial and error by fitting to experimental results. Once the micromechanical properties are fixed, a parametric study is possible by varying e.g. the fibre content or fibre length.

Key words: **Composite, fibre, brittle, finite element method, smeared crack model, discrete crack model**

1 Introduction

Fibres can be used in brittle materials to enhance the post-cracking behaviour. The cracking stress may also increase, but usually the main effect of fibres is observed after cracking, with fibres bridging the crack. If properly designed, the composite may also reach the process of multiple cracking and exhibit thereafter a strain-hardening behaviour.

Short fibres in the composite are more or less uniformly distributed. Thus the material can be considered homogeneous. Fibres are not modelled separately, but the constitutive relation takes them into account in a statistical manner. In this study, a numerical model is used to compute the composite tensile behaviour. A fibre analysis is performed to compute the contribution of a single fibre [1,2], and the macro-mechanical tensile behaviour is obtained by integrating over all fibre locations and orientations [3,4].

In order to analyse complex structures under a multi-axial stress state, the tensile model must be extended to two or three dimensions. This extension is generally a very complex one. In case of

---

* On leave from VTT Building Technology, P.O. Box 18071, FIN-02044 VTT, Finland.
HERON, Vol. 42, No. 1 (1997) ISSN 0046-7316

fibre-reinforced brittle materials, solutions to the problem already exist. Because the behaviour is similar to that of semi-brittle materials like concrete, the cracking and tensile softening relation being the main phenomena, the same methods can be used as with plain concrete. The material properties should only be refined. Initially, the material can be considered homogeneous and linear elastic. After cracking it becomes highly non-linear and orthotropic, having different properties normal and parallel to the crack.

Some of the methods most used for analysing cracking materials include the smeared and discrete crack approaches [5]. If the stress state is a combination of tension and compression, a multi-surface plasticity model can be used, with a yield condition of Rankine for the tensile regime and Von Mises or Drucker-Prager yield condition for the compressive regime [6]. In order to analyse structures made from fibre-reinforced brittle materials, a general purpose finite element program is needed which includes algorithms for cracking. The finite element package DIANA is used in this study.

The smeared crack approach is widely used because it fits the nature of finite elements, i.e. having continuity of the displacement field. Moreover, the locations of the cracks are usually not known in advance. The method can, however, suffer from stress locking and thus over-estimates the strength and stiffness [5]. Therefore, Rots [5] and Rots and Blaauwendraad [7] suggest using the smeared approach as a predictor, while the corrector analysis is made using a discrete crack concept.
The discrete crack approach has been found to give better results than the smeared crack concept, because the cracks are modelled correctly as geometrical discontinuities. Interface elements of zero thickness are used for the modelling of cracks. However, the problem with discrete cracks is the difficulty of generating the interface elements. If a predictor analysis is performed with a smeared crack concept, the element mesh has to be refined for the discrete crack analysis. Hence, the geometry must be modelled twice to get accurate results. This may lead to low utilization of the otherwise superior discrete crack concept. In this study, this obstacle is partly removed by automatic creation of discrete cracks on the existing geometry.

Structures analysed in the present study include beams without an ordinary reinforcement, a reinforced beam where fibres replace the stirrups, and a concrete pipe. Experimental results can be found from the literature.

2 Modelling strategies

2.1 *Smeared crack concept*

The smeared crack concept uses ordinary continuum elements for modelling structural discontinuities. After initiation of the crack, anisotropic material properties are assigned to the element. In case of cracking, the most important behaviour is in the direction normal to the crack. The shear stiffness is modelled with a shear retention factor [5]. The normal and shear stiffnesses of the crack are usually assumed to be uncoupled.

An important parameter in the smeared crack analysis is the characteristic length, or the crack band width, over which the microcracks are assumed to be uniformly spread. In structural elements, the characteristic length depends on the element size in the direction normal to the crack. With this approach, the results are objective with regard to mesh refinement. However, the objective fracture energy may not be obtained if the element size is too large [8]. Characteristic width has been studied by Bažant and Oh [8], who connected it to the area of element A and the orientation of crack α: $h = \sqrt{A}/\cos\alpha$; Rots [5], who used a predefined value of $h = \sqrt{2A}$ for linear two-dimensional elements, which is independent of the crack orientation; Dahlblom and Ottosen [9], who defined it geometrically as the distance between outermost nodes in the direction normal to the crack; and Oliver [10], who derived a consistent characteristic length for 3- and 4-node elements. In the present study the DIANA software is used, which allows a multi-linear stress-strain relation normal to the crack [6]. In order to obtain the crack strain, the crack opening must be divided by the characteristic length, which must therefore be approximated before analysis. In this study linear elements are used, hence the characteristic length can be prefined as the element length in the direction normal to the expected crack.

2.2 *Discrete crack concept*

In a discrete crack approach, the discontinuities are modelled with interface elements. Because interface elements have pairs of overlapping nodes, their initial stiffness is assigned a large value in order to simulate the rigid uncracked state. After cracking the overlapping nodes separate according to the constitutive relationship between the stress and the crack opening. The choice of the integration scheme affects considerably the performance of the interface elements [5]. When using a large value for the initial stiffness, Gauss integration is not recommended because of significant oscillations [5]. A lumped integration scheme yields better results and should be preferred.

2.3 *Combined plasticity model*

In analyses with a bi-axial stress state, the modelling of tension and compression with smeared cracking and plasticity models respectively may lead to numerical oscillation [6]. Therefore, alternative plasticity models for combined tension and compression have been developed which can be solved with stable algorithms. The tensile regime is described by the Rankine yield condition, while the compressive regime is described by another yield condition, either Von Mises or Drucker-Prager [6] (Figure 1). The tensile behaviour in these models resembles the rotating smeared crack concept [11]. The rotating crack approach has been reported by Willam et al. [12].

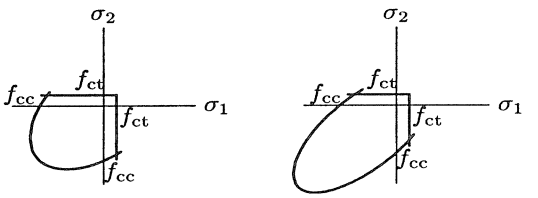

(a) Rankine/Von Mises *(b) Rankine/Drucker-Prager*

Fig. 1. Combined plasticity models for brittle materials [6].

2.4 *Generation of interface elements*

If a predictor analysis using a smeared crack approach is performed, the crack locations are available. Moreover, the geometry already exists, only the discrete cracks needing to be modelled. In order to avoid the total process of re-modelling, a method to generate cracks on an existing mesh is developed.

The method originates from a problem of modelling stiffened shell structures, e.g. ship decks [13]. The main idea is that when an arbitrary line crosses the existing element mesh, the elements along the line are divided. If cracks are to be modelled, the element boundaries must be separated on either side of the line and connected with interface elements. The algorithm can also be used in an ordinary modelling of the main geometry. The main restriction is that the method works for planar models only.

```
*NODES
290  0.00 0.017
291   0.16 0.017
*CRACK
17  170
12    80  299
7  58
*REBAR
290  291
```

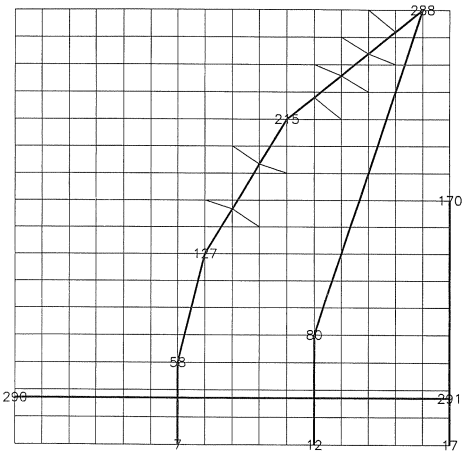

Fig. 2. Automatic generation of discrete cracks, reinforcing bars and bond-slip elements on a regular mesh. Thick lines represent cracks or reinforcement. The definition of objects and corresponding nodes are plotted.

The ordinary reinforcement can be modelled with a slightly modified routine. The mesh is first split and the reinforcement bars thereafter created with interface elements connecting them to the plane elements. These interface elements are used to represent the bond-slip behaviour.

An example of automatic generation of discrete cracks, reinforcing bars, and bond-slip elements on an existing regular mesh is shown in Figure 2. The mesh splitting algorithm tries to create quadrilaterals whenever possible, otherwise triangular elements are generated. Moreover, new nodes are only created at points where the line crosses the element boundary. Based on the same algorithm, different objects can be created. For example, holes, the outer boundary, cracks, reinforcement bars, or a normal element mesh can be defined with lines. The lines can be quite arbitrary, and may also cross, which enables the generation of several cracks in a single point. Figure 2 shows how easily the interface elements and reinforcing bars can be generated on an

existing geometry. However, the shape of the elements in the vicinity of the line is not always as regular as desired. It is believed that much work can be saved and many mistakes avoided when using the proposed method.

2.5 *Crack parameters*

Depending on the fracture mode, there are different possibilities to model the crack behaviour of fibre-reinforced brittle materials. If the composite fails in a single fracture mode, the tension softening curve can be used in the same manner as in the case of plain concrete [5, 8]. Hence, when using the smeared crack concept, the crack width must be divided by a characteristic length h.

In case of a strain-hardening composite failing in multiple fracture, the modelling is more complicated. When incorporating the constitutive relations into a finite element analysis, scaling according to the element size should be executed only for terms including the characteristic length h (see Figure 3). At the strain hardening stage, the strain consists of the average matrix strain $\overline{\varepsilon_m}$ and the crack width w: $\varepsilon_c = \overline{\varepsilon_m} + w/2s$, both components of which can be interpreted as true strains in subsequent analyses. The strain no longer depends on the element size, but on the crack spacing $2s$, thus being a material property. If using the discrete crack approach, the crack width depends on the selected crack spacing, so that in tension the elongation would become equal to that with the true crack spacing.

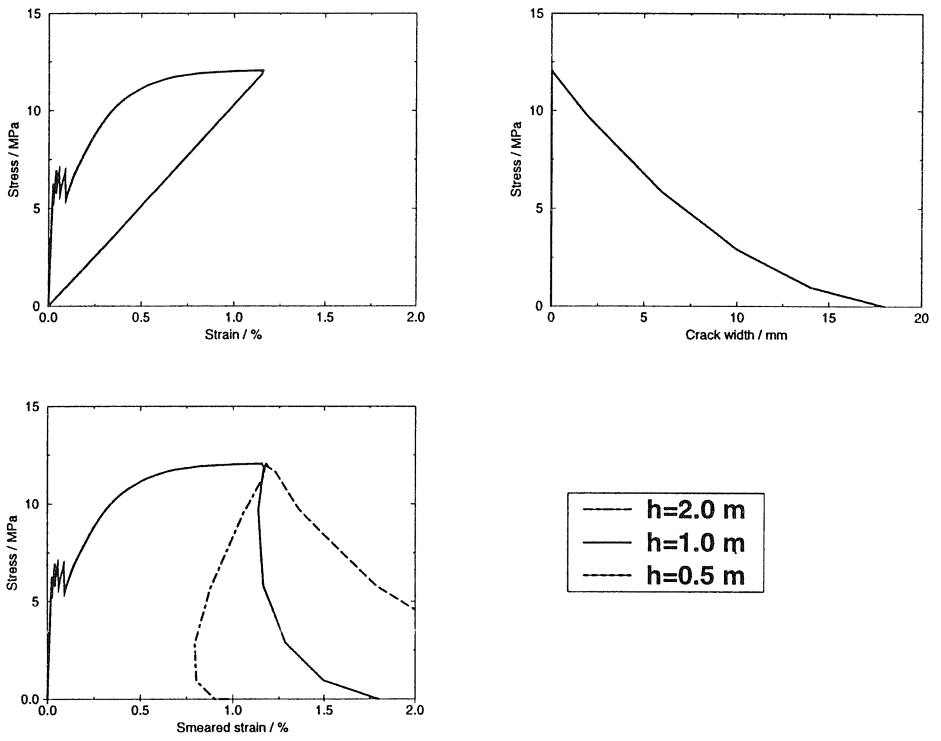

Fig. 3. Tensile hardening and softening relations for multiply cracked material.

During crack localization in the multiply cracked stage, the strain comprises three terms: $\varepsilon_c = \overline{\varepsilon_m} + w_{ul}/2s + w_{loc}/h$, where w_{ul} is the width of the unloading or closing cracks equal for all cracks, and w_{loc} is the additional localized crack width. The total width of the opening crack is then $w_o = w_{ul} + w_{loc}$. If using the discrete crack approach, the opening crack can simply be modelled with a tension-softening curve ($\sigma - w_0$). One possibility is to use a smeared crack approach for the strain-hardening case, while the crack localization ($\sigma - w_{loc}$) is taken into account by discrete cracks, which start to open only beyond the peak. When using the smeared crack concept, it can be seen that only part of the crack width depends on the characteristic width h, while the rest is independent of the element size (see Figure 3).

In DIANA the total strain is decomposed into elastic and crack strains [5]. Therefore, from the composite strains above, the elastic strain should be subtracted before incorporating into the model.

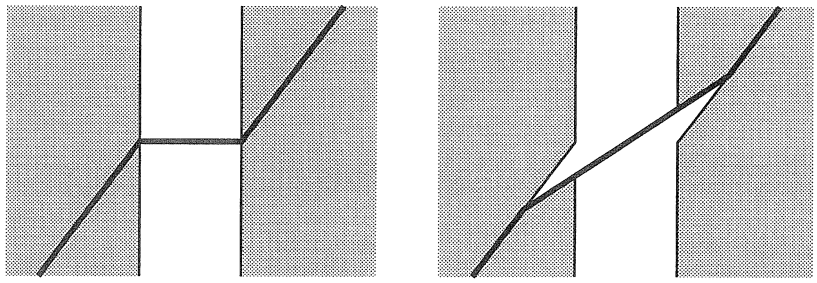

a) *b)*

Fig. 4. Fibre position at the crack: a) normal to the crack, and b) inclined due to matrix spalling.

The behaviour normal to the crack can be derived from the uniaxial tensile model. This crack bridging action is assumed to be the main effect of fibres, while the shear stiffness of an open crack is assumed to be negligible. This choice is justifiable, at least with proportional loading. The crack forms perpendicular to the major principal stress (tensile stress positive). Hence, at the onset of cracking the crack shear stress is zero. Therefore, the mode I behaviour is probably much more significant than the mode II stiffness. In addition, if the fibres at a crack are aligned normal to the crack face, and they are assumed completely flexible, the assumption of zero shear stiffness is justified. However, if matrix spalling occurs, it affects an inclined position of fibres at the crack, increasing the shear stiffness (Figure 4). Moreover, at low crack widths the aggregate interlock effect may be significant. This effect is, however, neglected in the present study, where large crack openings may occur due to fibres bridging the crack. The spalling effect is also neglected as none of the materials considered in the present study are assumed to exhibit matrix spalling.

3 Applications

The behaviour of different structures under a two-dimensional stress or strain state is computed using the DIANA finite element software. The studied materials include various fibre-reinforced

cementitious materials. The results are then compared with the experiments found in the literature. The mode I crack behaviour is computed from micromechanical properties using a micromechanical statistical tensile model [1,3]. Some micromechanical parameters were not reported and are therefore approximated by trial and error to fit the experiments.

3.1 *FR-DSP beams*

Tjiptobroto and Hansen [14] studied the bending behaviour of beams with four-point loading, using different amounts of short steel fibres. The material is called fibre-reinforced densified small particles (FR-DSP). Beam dimensions of $50 \times 50 \times 500$ mm and a span of 420 mm were used. The material properties used in the calculations are, for the matrix: modulus of elasticity $E_m = 49.1$ GPa, cracking stress σ_{mu} varies with V_f; for steel fibres: modulus of elasticity $E_f = 200$ GPa, volume content $V_f = 3$, 6, 9, and 12%, diameter $d_f = 0.15$ mm, length $l_f = 6$ mm, and tensile strength $\sigma_{fu} = 2950$ MPa; for the interface: shear strength $\tau_u = 6$ MPa, frictional shear stress $\tau_f = 4$ MPa, and debonding fracture energy $G_{db} = 150$ N/m.

A high value of interface shear fracture energy ($G_{db} = 120$ N/m) was approximated by Tjiptobroto and Hansen [14] to explain the strain-hardening behaviour. Computing the constitutive behaviour normal to the crack, an interface shear strength of $\tau_u = 6.0$ MPa was chosen. The frictional shear stress then decreases linearly from that value to $\tau_f = 4$ MPa, with a slip of 0.15 mm, resulting in $G_{db} = 150$ N/m. Thereafter, the frictional shear stress is kept constant.

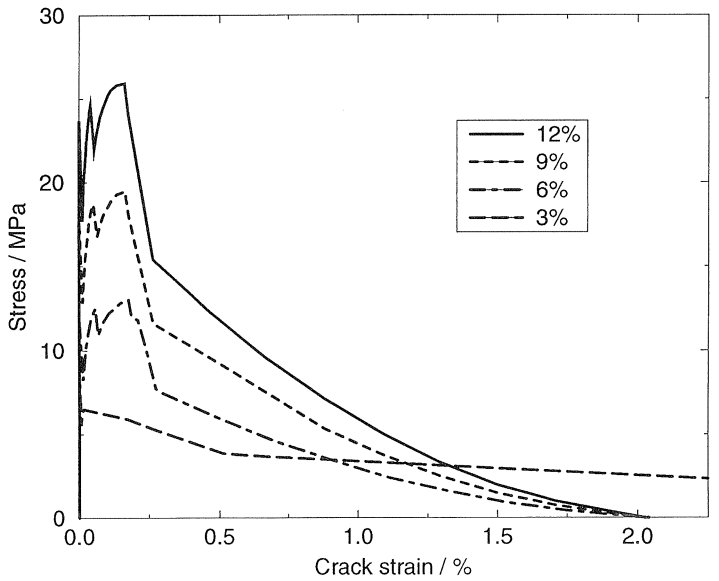

Fig. 5. Computed tensile stress-strain relations with different fibre contents.

The cracking stress is proportional to $V_f^{2/3}$ according to Aveston et al. [15]. If the cracking stress is 8.0 MPa with 3 vol.-% of fibres, values of 12.7, 16.6, and 20.0 MPa are obtained with 6, 9, and 12% of fibres, respectively. The stress-strain relations normal to the crack were computed from micro-mechanical properties [1, 3] and are shown in Figure 5 for different fibre contents. Multiple fracture was predicted for all fibre contents, except with $V_f = 3\%$, which fails in a single fracture mode. This is in agreement with the result of Tjiptobroto and Hansen [14], who approximated the critical fibre volume fraction as 3.8%.

The compression zone is assumed to be linear elastic. With the highest amount of fibres ($V_f = 12\%$), it is possible that the stress exceeds the compressive strength of 175 MPa. However, this is not taken into account in this study.

Only half of the structure was modelled with three-noded beam elements with 15 integration points (Simpson rule) along the beam height, and two (Gauss integration) along the axis (see Figure 6). The span between the loading points was modelled as a single element, because of a constant moment. Only with the fibre volume content of $V_f = 3\%$ were four elements used in the constant moment region. Because of single fracture, only the element at the symmetry axis is allowed to crack. From the support to the loading point, five elements were used.

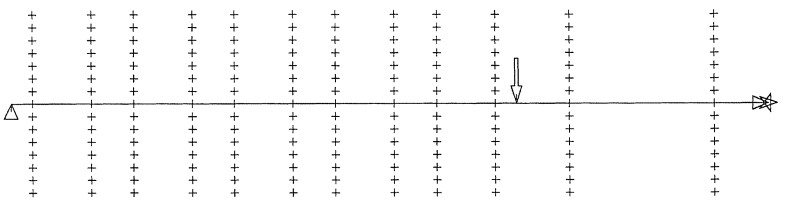

Fig. 6. Beam model with integration points.

The experimental and computed load-midpoint displacement relations of the beam are shown in Figure 7. The agreement is good; only with the lowest fibre content is the peak predicted at too low a strain. With the highest fibre content $V_f = 12\%$, the maximum load level was reported to be 14 kN, although in Figure 7 it is higher.

The present analysis shows the applicability of simple beam elements and a smeared crack approach to reproduce the flexural behaviour of beams failing in a multiple fracture mode.

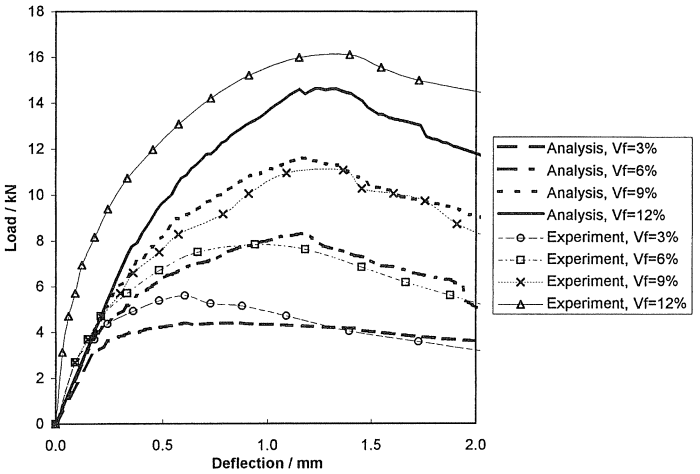

Fig. 7. Experimental [14] and computed load-displacement curves for FR-DSP *beams with different fibre volume contents.*

3.2 *Mortar beams reinforced with aramide fibres*

Ward and Li [16] studied the flexural behaviour of fibre-reinforced mortar beams. They performed flexural tests with various fibre types and volume fractions on three different beam sizes, the geometry of the beam remaining the same, with beam depth d, width $b = 0.55d$, and span $l = 3d$. Aramide (kevlar) fibres were chosen for the present study.

The material properties used in calculations are, for the matrix: modulus of elasticity E_m=31 GPa, tensile strength $\sigma_{mu} = 1.8$ MPa and fracture energy $G_m = 50$ N/m; for aramide fibres: modulus of elasticity $E_f = 130$ GPa, volume fraction $V_f = 0$, 0.5, 1.0, and 1.5%, diameter $d_f = 0.0136$ mm, length $l_f = 6.4$ mm, and tensile strength $\sigma_{fu} = 2800$ MPa; for the interface: bond modulus $\kappa = 5 \cdot 10^{13}$ N/m^3, shear strength $\tau_u = 0.6$ MPa, frictional shear stress $\tau_f = 0.25$ MPa, and debonding energy $G_{db} = 50$ N/m.

The cracking stress may increase with increasing fibre volume content [15]. If the tensile softening diagram of the matrix is added to the diagram of fibre pull-out, the peak appears at 1.96, 2.60, and 3.25 MPa with fibre contents of 0.5, 1.0, and 1.5%, respectively. The computed stress-crack opening relations are shown in Figure 8.

Only half the beam is modelled due to the symmetry. Four-noded plain stress elements are used. The element model is shown in Figure 9. Because the material fails in a single fracture mode in tension, only a single discrete crack is modelled on the symmetry axis. Four-noded interface elements with a lumped integration scheme are used to model the crack. The plane stress elements are linear elastic.

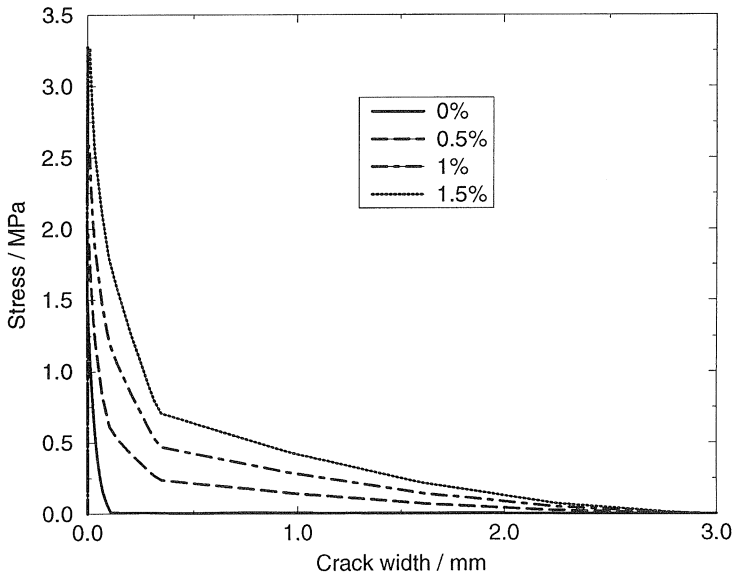

Fig. 8. Computed tensile stress-crack width relations for plain and aramide fibre-reinforced mortar with different fibre volume contents.

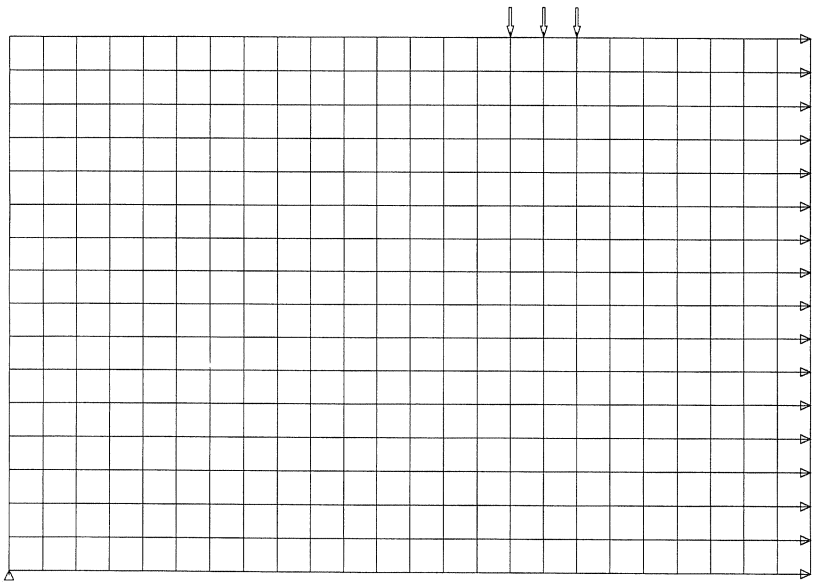

Fig. 9. Element model for fibre-reinforced mortar beams.

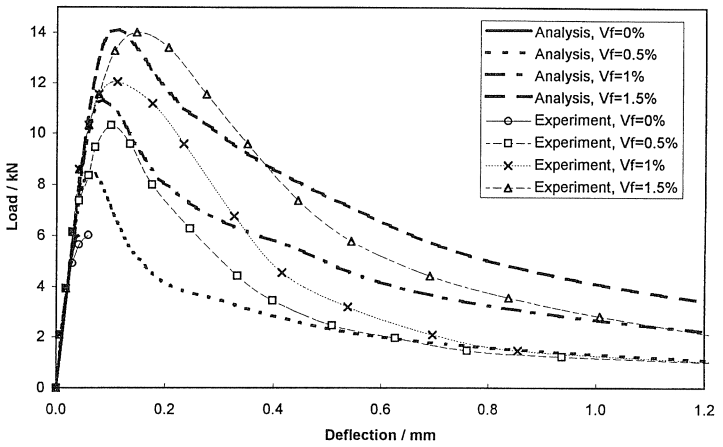

Fig. 10. Experimental [16] and computed load-deflection curves for kevlar fibre reinforced beams with different fibre contents.

The experimental and computed load-deflection curves are shown in Figure 10 for beam depth $d = 114$ mm. It can be seen that the peak is correctly predicted for the highest fibre content, whereas for other fibre volume fractions the computed peak load is too low. The discrepancy increases as the fibre content decreases. For plain concrete the tensile strength was adjusted to fit the experiments. Therefore, a low strength (1.8 MPa) is used, while a splitting tensile strength of 2.9 MPa was reported. It can be seen, however, that in the experiments the plain concrete beam exhibits a more ductile behaviour than that computed. Too steep a computed tensile softening relation of the plain concrete is therefore a possible source of the discrepancy also with low fibre contents.

In the study by Ward and Li [16], different beam sizes were tested with a kevlar fibre volume content $V_f = 1.5\%$. The beam depths used in the experiments were $d = 114$, 171, and 228 mm. The tensile softening relation shown in Figure 8 was used in the computations. The experimental and computed flexural stress-normalized deflection relations are shown in Figure 11. The normalized load is defined as $6M/bd^2$, where M is the bending moment along the constant moment span and b is the beam width. The normalized deflection is defined as the midspan deflection divided by the beam depth. Figure 11 shows that the correct size effect can be predicted, provided that a proper tensile softening relation is used.

The present analysis introduces an increase in peak load with increasing fibre content, when the structure fails in a single fracture mode, exhibiting a more ductile tensile behaviour than the plain mortar. Moreover, the computations resulted in a similar size effect to that in the experiments.

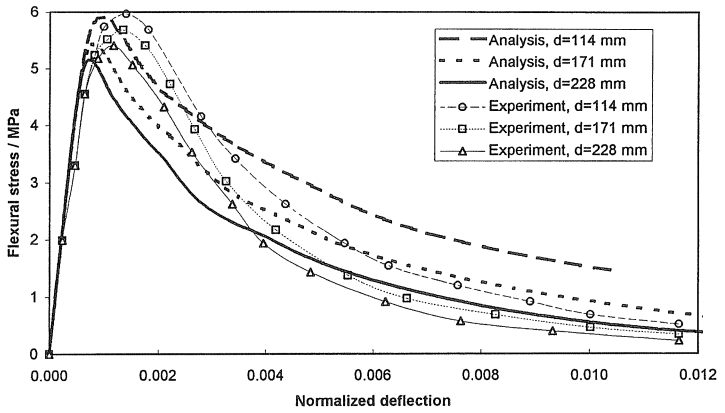

Fig. 11. Experimental [16] and computed flexural stress versus normalized deflection for different sizes of beam reinforced with 1.5 vol.-% kevlar fibres.

3.3 *Fibres as shear reinforcement*

One potential application is to replace the stirrups in structural beams by fibres. Several researchers have studied this possibility and semi-empirical or analytical formulae have been suggested to predict the ultimate shear strength [17-23]. The purpose of the present section is to study whether the shear strength is possible to predict by the finite element method. Li et al. [17] studied experimentally the behaviour of mortar beams with fibres as shear reinforcement. The same materials were used as by Ward and Li [16], but with additional steel bars as ordinary reinforcement. The peak loads were given, but no load-deflection curves. Narayanan and Darwish [21] performed similar tests with steel fibres and reported typical crack patterns as well as a comparison between fibre and stirrup concrete beams.

Based on Li et al. [17] a structure is chosen with an effective depth d = 102 mm, shear span a = 306 mm, and reinforcement ratio ρ = 2.2%, with a centre-point loading. The structure is modelled with four-noded plane stress elements. The reinforcement is located 25 mm above the bottom of the beam, and is modelled with truss elements of cross-sectional area equal to that of the two steel bars of diameter 9.53 mm. The yield stress of the bars is 450 MPa and the ultimate strength 700 MPa. The truss elements are connected to the main structure with interface elements representing the bond-slip behaviour. The reinforcement is continuous also across cracks as illustrated in Figure 12. It should be noted that the opposite nodes of interface elements overlap; the gap is plotted only for clarity. In a combined plasticity approach, no discrete cracks appear. Hence, the crack nodes in Figure 12 coincide. The bond-slip between the reinforcement and mortar is modelled using the relation by Dörr available in DIANA [6].

As suggested by Rots [5], a smeared crack analysis is performed first to predict the crack position and direction of the dominant cracks. In fact, a combined plasticity model is used with the Rankine and the Von Mises yield conditions for the tensile and compressive regimes, respectively. The crack

patterns and incremental displacements near the peak with and without fibres are shown in Figures 13 and 14, respectively. The computed load-deflection relations are shown in Figure 15. For a plain mortar beam, a peak stress with a localized shear crack could be obtained, whereas the fibre-reinforced beam is predicted to fail by yielding of reinforcement, which is not reported for this beam. The inability of the smeared crack approach to trace the shear failure was also reported by Rots et al. [24]. Therefore, a discrete crack corrector analysis is performed. For both materials the model shown in Figure 16 is used. The discrete cracks, reinforcing bars, and the bond-slip elements are created using an automatic routine, which makes the corrector analysis more tempting and available.

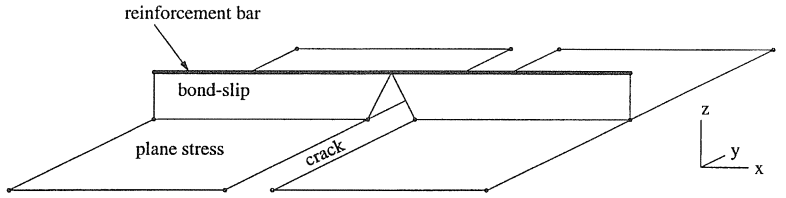

Fig. 12. Modelling of crack, bond-slib and reinforcement.

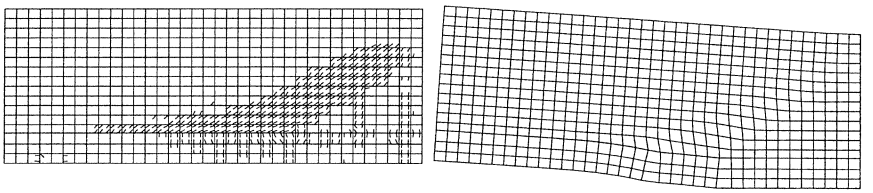

a) *b)*

Fig. 13. Combined plasticity analysis of reinforced beam without shear reinforcement. a) Crack pattern, and b) incremental displacements near the peak.

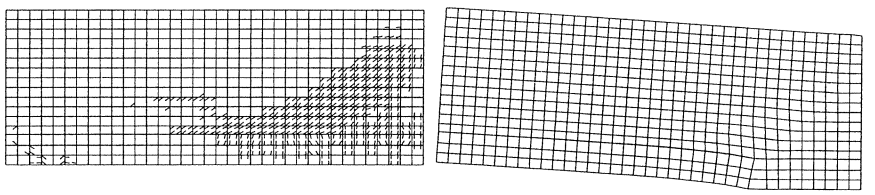

a) *b)*

Fig. 14. Combined plasticity analysis of reinforced beam with 1 vol.-% kevlar fibres as shear reinforcement. a) Crack pattern, and b) incremental displacements before yielding of reinforcement.

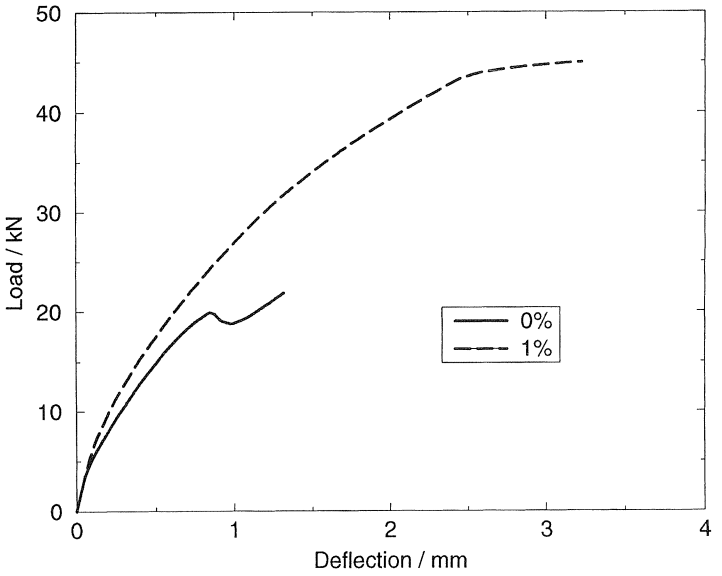

Fig. 15. Load-deflection curves from combined plasticity analyses of reinforced beams with and without fibres.

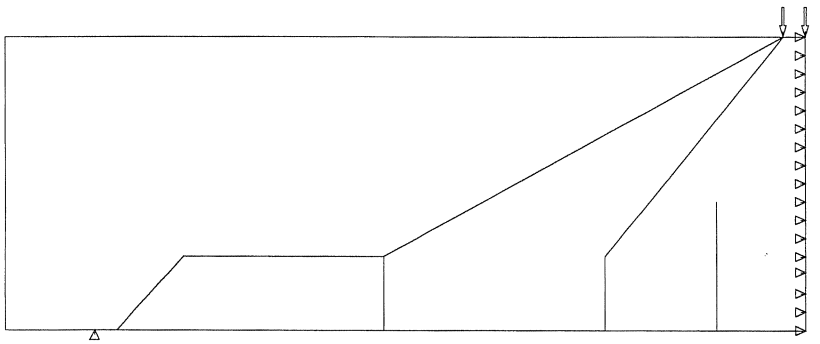

Fig. 16. Position of discrete cracks.

The analysis itself, however, had to be performed carefully to obtain a convergent solution. In the present study an indirect displacement control was used [6] where only the crack opening displacements of the inclined crack are considered in an arc-length method. With this control method the snap-back could be traced. It was possible to obtain a convergent solution, with a variation of 10^{-4} on the reference energy norm. An automatic or constant load incrementation was not possible, but at different stages the load increments had to be selected by trial and error.

The incremental displacements beyond peak load are shown in Figure 17 without dowel action and with infinite dowel stiffness. The computed load-deflection relations are shown in Figure 18. The ultimate loads derived from different analyses and the experimental peak loads are shown in Table 1. In the study by Li et al. [17] some cracks were seen to propagate along the reinforcement, and ultimate failure occurred by breakdown of the dowel action. It can be seen that with a plain mortar the peak load agrees better with experiments when using an infinite dowel action, whereas with fibres a correct peak load is obtained without dowel action. With dowel action the beam is predicted to fail by yielding of reinforcement. Feenstra et al. [25] neglected the dowel action in a reinforced concrete beam and obtained a 18% lower peak load than in the experiments. However, the study of the dowel action is beyond the scope of this study.

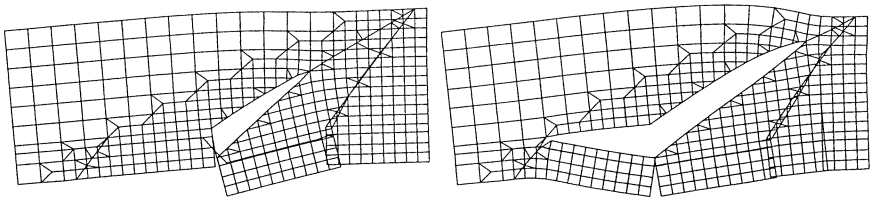

a) *b)*

Fig. 17. *Discrete crack analysis of reinforced beam. Incremental displacements beyond peak, with a) zero dowel action, and b) infinite dowel stiffness.*

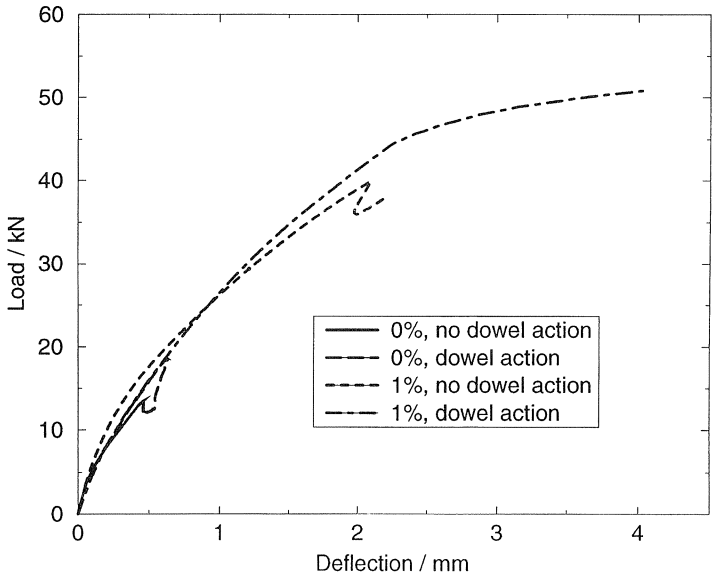

Fig. 18. *Load-deflection curves from discrete crack analyses of reinforced beams with and without fibres.*

Table 1. Peak loads of reinforced beams using different modelling strategies.

V_f / %	combined plasticity	discrete, no dowel action	discrete, dowel action	experiment
0	19.9	13.5	18.6	20.8
1	45*	39.9	50*	39.2

* flexural failure

Narayanan and Darwish [21] observed the failure mode to change from shear failure to flexural-shear failure, and further to flexural failure as the fibre volume fraction increased. With a low fibre content, the crack propagated along the main reinforcement. However, with higher fibre contents, the crack pattern changed to the flexural type of failure. This observation supports the computed results, with a high dowel stiffness for the plain mortar, and a low stiffness with fibres.

The method seems to be promising, but further research should be done to correctly analyse the ultimate load as well as the fracture mode. An increase in peak load due to fibres could be derived, and thus the influence of the fibres acting as shear reinforcement can be physically explained. The obstacle in re-modelling the geometry for a corrector discrete crack analysis has been overcome, but there remain problems for further study. The dowel action, which is probably a non-linear interaction between the reinforcement and the concrete, should be adequately modelled. Without a proper dowel action model available, it is safer to neglect the dowel stiffness. In addition, analysis control routines should be refined to make them more automatic and part of engineering practice.

3.4 *Concrete pipes*

Schipperen [26] performed numerical analyses of small-diameter FRC pipes, observing that a completely plastic model for Dramix fibres leads to a nice resemblance to the experimental results. In the following, an explanation is given using the micromechanical model. The analysis is also performed for plain concrete as well as Wirex fibre-reinforced concrete pipes.

In the tests, a pipe with an outer diameter 1000 mm, length 500 mm, and wall thickness 50 mm was subjected to a diametral line load. The material properties used in the calculations are, for the matrix: modulus of elasticity $E_m = 30$ GPa, cracking stress $\sigma_{mu} = 2.2$ and 2.0 MPa with and without fibres, respectively, and mode I fracture energy $G_m = 65$ N/m; for Dramix fibres: modulus of elasticity $E_f = 210$ GPa, volume fraction $V_f = 1.2\%$, diameter $d_f = 0.8$ mm, length $l_f = 60$ mm, and for the interface: shear strength $\tau_u = 6$ MPa, and frictional shear stress $\tau_f = 5$ MPa; for Wirex fibres: modulus of elasticity $E_f = 210$ GPa, volume fraction $V_f = 1.2\%$, diameter $d_f = 0.6$ mm, length $l_f = 40$ mm, and for the interface: shear strength $\tau_u = 4.5$ MPa, debonding energy $G_{db} = 50$ N/m, and frictional shear stress $\tau_f = 2.5$ MPa.

Because of a high fibre length with respect to the wall thickness, the fibres are assumed to have a two-dimensional random distribution. The computed stress-crack opening relations are shown in Figure 19. The tension softening curve for plain concrete is hardly noticeable, since the critical crack opening displacement is very low compared with that of the fibre-reinforced concrete, for which it equals half the fibre length due to pull-out of the shorter embedded length. Dramix fibres have hooked ends, the effects of which is approximated by using a high value for the interfacial shear stress.

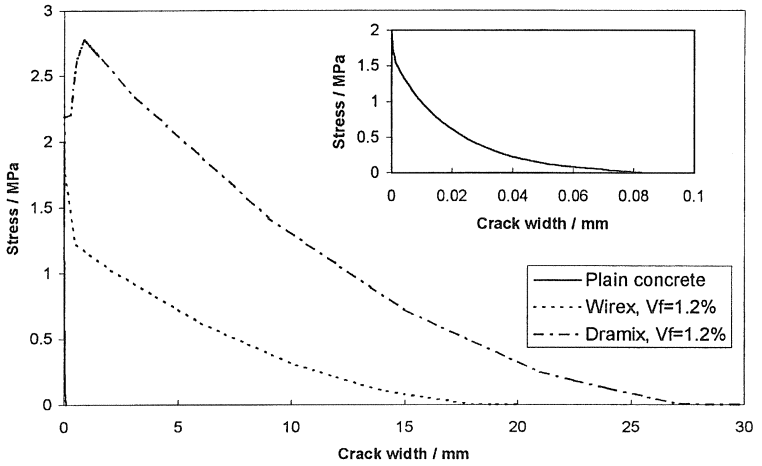

Fig. 19. Computed tensile stress-crack opening relations with different steel fibres.

At the onset of cracking the stress first drops, but begins to increase again due to the fibre pull-out action. With Dramix fibres, the post-cracking strength exceeds the cracking stress, indicating steady-state cracking at constant stress followed by multiple cracking. The constitutive model [3] gives a crack spacing of 30 mm. Because the main effect is due to crack localization, only a single crack is modelled, leading to a somewhat stiffer response than that if multiple fracture were considered. Beyond post-cracking peak, fibres are pulled out resulting in a slowly descending curve. The slope is so low that for crack widths up to, say 2 mm, the stress can be considered almost constant. This is why the plasticity model works in this case, although it does not give physical insight. Therefore, it should be used with care. The present model, on the other hand, is based on physical phenomena, and should be preferred.

Only a quarter of the structure is modelled with four-noded plain strain elements. The element model is shown in Figure 20. Discrete cracks are modelled with four-noded interface elements on both axes of symmetry. A two-node Newton-Cotes integration scheme is used. The rest of the structure behaves in linear elastic mode.

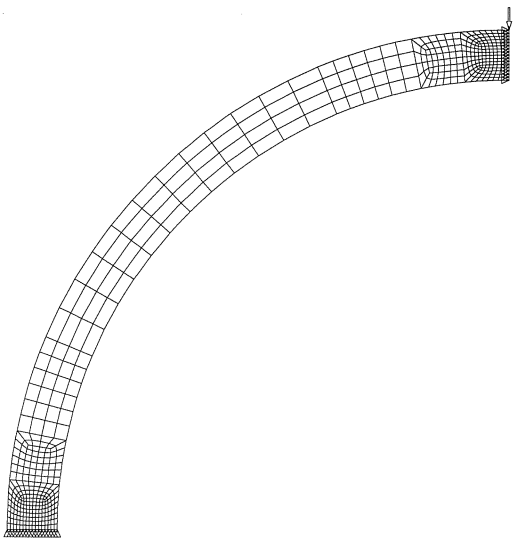

Fig. 20. Quarter model of a concrete pipe.

The experimental and computed load-diameter decrease relations are shown in Figure 21. The increase in both peak load and the ductility of the pipe due to fibres is clearly be visible. The agreement between the computed and experimental results is rather good. In the analysis of the plain concrete pipe, two cracks appear simultaneously because of assumed symmetry, resulting in two peaks instead of four found in experiments [26]. Nevertheless, a correct peak load could be reproduced.

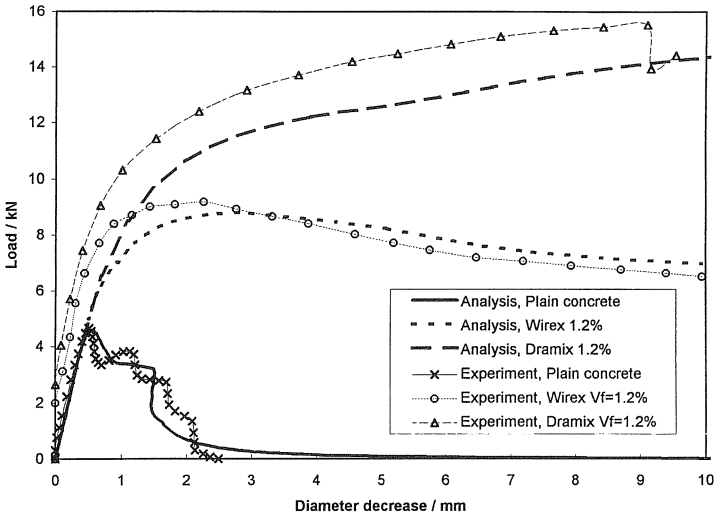

Fig. 21. Experimental [27] and computed load versus diameter decrease for pipes with no fibres, 1.2 vol.-% Wirex fibres, and 1.2 vol.-% Dramix fibres.

4 Summary and conclusions

Smeared and discrete crack approaches have been used to analyse the behaviour of fibre-reinforced structures under two-dimensional stress or strain state. The behaviour after cracking is governed by the crack normal behaviour, which is computed from micro-mechanical properties. The crack shear effect is assumed to be negligible.

In all problems analysed the enhancement due to fibres was captured, with good correspondence to experimental results. Moreover, a correct size effect of beams could be reproduced. This supports the validity of the analysis methods for these materials, at least in case of flexural members subjected to a proportional loading. The effectiveness of fibres in a bi-axial stress state were seen to be due mainly to the action normal to the crack. More detailed crack models could also be used, with a shear stiffness or coupling between the normal and shear stiffnesses. These may not, however, considerably affect the results.

In a more complex problem, a reinforced beam with fibres as shear reinforcement was first analysed with a combined plasticity model as a predictor and thereafter using the discrete crack approach as a corrector. The snap-back behaviour could only be captured with the discrete crack approach. Due to convergence problems this analysis was seen to be beyond normal engineering practice. More research is needed to overcome this challenge. However, the effect of fibres as shear reinforcement could be clearly obtained.

Because the crack tensile behaviour was computed from micromechanical properties, further analyses can be made by varying some parameters while keeping the others fixed. For example, the effects of increasing the fibre content or fibre aspect ratio can be studied.

Acknowledgements

This study was carried out in the Netherlands, at Delft University of Technology, Faculty of Civil Engineering, and at TNO Building and Construction Research as part of a European Community research training project "Constitutive modelling of fibre-reinforced brittle materials for numerical analysis" under the programme "Training and Mobility of Researchers" financed by the European Commission.

I would like to express my sincere gratitude to my hosts in Delft, Professor Johan Blaauwendraad at the Delft University of Technology, and Dr. Jan Rots at TNO Building and Construction Research. Moreover, I wish to thank Dr. Peter Feenstra for his valuable comments.

References

1. KULLAA, J. 1997a. Micromechanics of multiple cracking. Part I: Fibre analysis. Submitted to Journal of Materials Science.
2. KULLAA, J. 1996. Micromechanics of multiple cracking. Crack Bridging. TUD report 03.21.0.22.21, Delft University of Technology, Faculty of Civil Engineering, Delft. 52p.
3. KULLAA, J. 1997b. Micromechanics of multiple cracking. Part II: Statistical tensile behaviour. Submitted to Journal of Materials Science.
4. KULLAA, J. 1997c. Micromechanics of multiple cracking. Statistical tensile behaviour. TUD report 03.21.0.22.40, Delft University of Technology, Faculty of Civil Engineering, Delft. 54 p.
5. ROTS, J.G. 1988. Computational modeling of concrete fracture. PhD thesis. Delft University of Technology, Delft, The Netherlands. 129 p.
6. DIANA - Finite element analysis. User's manual release 6.1. Nonlinear analysis. TNO Building and Construction Research, Delft, The Netherlands (1996).
7. ROTS, J.G. and Blaauwendraad, J. 1989. Crack models for concrete: Discrete or smeared? Fixed, multi-directional or rotating? HERON, Vol. 34, No. 1, 1-59.
8. BAŽANT, Z.P. and OH, B.H. 1983. Crack band theory for fracture of concrete. Materials and Structures, RILEM, Vol. 16, No. 93, 155-177.
9. DAHLBLOM, O. and OTTOSEN, N.S. 1990. Smeared crack analysis using generalized fictitious crack model. Journal of Engineering Mechanics, Vol. 116, No. 1, 55-76.
10. OLIVER, J. 1989. A consistent characteristic length for smeared cracking models. International Journal for Numerical Methods in Engineering, Vol. 28, 461-474.
11. FEENSTRA, P.H. 1993. Computational aspects of biaxial stress in plain and reinforced concrete. PhD thesis. Delft University of Technology, Delft, The Netherlands. 151 p.
12. WILLAM, K., PRAMONO, E. and STURE, S. 1987. Fundamental issues of smeared crack models. Proc. SEM/RILEM Int. Conf. on Fracture of Concrete and Rock. S.P. Shah and S.E. Swartz (Eds.), Soc. for Experimental Mechanics Inc., Bethel, CT, USA, 192-207.
13. KULLAA, J. and KLINGE, P. 1995. A geometry based generation of a finite element model for stiffened shell structures. Computers and Structures, Vol. 54, No. 5, 979-987.
14. TJIPTOBROTO, P. and HANSEN, W. 1993. Tensile strain hardening and multiple cracking in high-performance cement-based composites containing discontinuous fibers. ACI Materials Journal, Vol. 90, No. 1, 16-25.
15. AVESTON, J., COOPER, G. A. and KELLY, A. 1971. Single and multiple fracture. The Properties of Fibre Composites. Proc. Conf. National Physical Laboratories. 4 Nov. 1971. Guildford. IPC Science and Technology Press Ltd. 15-24.
16. WARD, R. and LI, V.C. 1990. Dependence of flexural behavior of fiber reinforced mortar on material fracture resistance and beam size. ACI Materials Journal, Vol. 87, No. 6, 627-637.
17. LI, V.C., WARD, R. and HAMZA, A.M. 1992. Steel and synthetic fibers as shear reinforcement. ACI Materials Journal, Vol. 89, No. 5, 499-508.
18. AL-TA'AN, S.A. and AL-FEEL, J.R. 1990. Evaluation of shear strength of fibre-reinforced concrete beams. Cement and Concrete Composites, Vol. 12, 87-94.
19. EL-NIEMA, E.I. 1991. Reinforced concrete beams with steel fibers under shear. ACI Structural Journal, Vol. 88, No. 2, 178-183.

20. Lim, T.Y., Paramasivam, P. and Lee, S.L. 1987. Shear and moment capacity of reinforced steel-fibre-concrete beams. Magazine of Concrete Research, Vol. 39, No. 140, 148-160.
21. Narayanan, R. and Darwish, I.Y.S. 1987. Use of steel fibers as shear reinforcement. aci Structural Journal, Vol. 84, No. 3, 216-227.
22. Sachan, A.K. and Kameswara Rao, C.V.S. 1990. Behaviour of fibre reinforced concrete deep beams. Cement and Concrete Composites, Vol. 12, No. 3, 211-218.
23. Tan, K.H., Murugappan, K. and Paramasivam, P. 1993. Shear behavior of steel fiber reinforced concrete beams. aci Structural Journal, Vol. 89, No. 6, 3-11.
24. Rots, J.G., Nauta, P., Kusters, G.M.A. and Blaauwendraad, J. 1985. Smeared crack approach and fracture localization in concrete. heron, Vol. 30, No. 1, 1–48.
25. Feenstra, P.H., de Borst, R. and Rots, J.G. 1991. Numerical study on crack dilatancy. II: Applications. Journal of Engineering Mechanics, Vol. 117, No. 4, 754-769.
26. Schipperen, J.H.A. 1994. Numerical research on steel fibre reinforced structures. tno/tud-report 94-CON-R0117/03.21.31.0.31, tno Building and Construction Research, Delft. 71 p.
27. Schulze, F. 1992. Results of the tests with small tubes under vertical loading. 5th meeting of Steering Committee of Brite-Euram project be-3275: Failure mechanics of fibre-reinforced concrete and pre-damaged structures. Gouda, the Netherlands, 18 September 1992 (unpublished).